^{31}P NMR (121.5 Hz) and ^{13}C NMR (75.5 MHz) spectra were recorded on a Bruker MSL 300 spectrometer and referenced relative to external trimethyl phosphate and dioxane, respectively. Two levels of broad band proton decoupling were applied for all the experiments. In the case of ^{31}P spectra, a Hahn spin echo sequence (90°–T–180°–T) was used with a T value of 1 ms in order to cancel the signal of membrane phospholipids whose transverse relaxation times (T_2) is less than 0.5 ms.

(33) Hore, P. J. *J. Magn. Reson.* **1983**, *54*, 539–542.

Acknowledgment. We thank Professor J. Igolen for his support and encouragement and Dr. A. Sanson for stimulating discussions. We also thank G. McCort and Dr. A. W. Rutherford for their help in the preparation of the manuscript.

Calculations of Charge-Transfer Transition Energies and Spectroscopic Properties of a Molecular Crystal: Methylbacteriopheophorbide *a*

William W. Parson,*,† Steven Creighton,‡ and Arieh Warshel*,‡

Contribution from the Department of Biochemistry, University of Washington, Seattle, Washington 98195, and Department of Chemistry, University of Southern California, Los Angeles, California 90007. *Received August 25, 1988*

Abstract: Theoretical expressions are developed for calculating the spectroscopic properties of molecular crystals. The theory is applied to crystalline methylbacteriopheophorbide *a* as a test case for a similar analysis of the properties of photosynthetic reaction centers. The treatment starts by writing π molecular orbitals for the individual molecules as linear combinations of atomic orbitals. Intermolecular interactions are included in the form of configuration interactions. Exciton-type interactions of intramolecular transitions are evaluated in terms of transition monopoles, and intermolecular charge-transfer (CT) transitions are included explicitly with the aid of semiempirical atomic resonance integrals and electron–electron repulsion integrals. The diagonal transition energies for the intramolecular transitions are obtained from the transition energies for a monomeric molecule in solution. CT transition energies are calculated by using experimentally measured reduction potentials in conjunction with calculations of electrostatic interactions in the crystal and in solution. This is done by taking into account the microscopic dielectric effect associated with the polarizabilities of the crystal atoms and by evaluating the solvation free energies of the oxidized and reduced molecules in solution. The calculated CT transition energies are close to the energies that are required to bring the calculated spectroscopic properties into alignment with the measured absorption spectrum and linear dichroism of the methylbacteriopheophorbide crystal. This is particularly encouraging, because no adjustable parameters are included in the construction of the crystal wave functions from those of the isolated molecules. The satisfactory agreement between theory and experiment lends support to attempts to calculate the spectroscopic properties and electron-transfer dynamics of photosynthetic reaction centers.

In previous papers,[1-4] we developed a quantum mechanical treatment of the spectroscopic properties and electron-transfer kinetics of reaction centers of photosynthetic bacteria. To evaluate the intermolecular interactions of the four molecules of bacteriochlorophyll and two molecules of bacteriopheophytin in the reaction center, the theory used semiempirical atomic resonance integrals and electron–electron repulsion integrals that had been parametrized in earlier studies of pyrene dimers and other excimers. Because the data set employed for this parametrization is limited, it is important to test the theory by applying it to oligomers of other molecules closely related to bacteriochlorophyll. Such a test will be most meaningful if the geometry of the oligomer is known accurately, because the resonance integrals are particularly strong functions of the molecular positions and orientations. One system that meets this criterion is crystalline methylbacteriopheophorbide *a* (MeBPh, Figures 1 and 2). Barkigia et al.[5] have solved the crystal structure by X-ray diffraction, and Hanson and Hofrichter[6] have measured the crystal's optical absorption spectrum and linear dichroism. The distances between neighboring MeBPh molecules in the crystal are similar to some of the intermolecular distances between bacteriochlorophylls in the reaction center, and some of the crystal's spectroscopic properties resemble those of the reaction center. In both cases, there is a strong absorption band at long wavelengths, shifted far to the red of the corresponding band in the spectrum of monomeric MeBPh or bacteriochlorophyll. An analysis of intermolecular charge-transfer (CT) transitions is more complicated for the crystal than for the reaction center, because each MeBPh molecule in the crystal has strong orbital overlap with a larger number of neighboring molecules. Exciton interactions among the pigments also extend over many more molecules in the crystal than in the reaction center. Nevertheless, a crystal provides a critical test case for calculations of the energetics of CT transitions in a well-defined environment.

The theory of optical absorption by molecular crystals was treated by Davydov for the case of a molecule with a single excited state or a set of noninteracting excited states.[7] In a more general situation the molecule will have a manifold of excited states that are mixed by intermolecular interactions, in addition to CT transitions that can mix with the intramolecular transitions.[8,9] We

† University of Washington.
‡ University of Southern California.

(1) Warshel, A.; Parson, W. W. *J. Am. Chem. Soc.* **1987**, *109*, 6123–6152.
(2) Parson, W. W.; Warshel, A. *J. Am. Chem. Soc.* **1987**, *109*, 6152–6163.
(3) Parson, W. W.; Creighton, S.; Warshel, A. In *Primary Processes in Photobiology*; Kobayashi, T., Ed.; Springer-Verlag: Berlin, 1987; pp 43–51.
(4) Warshel, A.; Creighton, S.; Parson, W. W. *J. Phys. Chem.* **1988**, *92*, 2696–2701.
(5) Barkigia, K. M.; Fajer, J.; Smith, K. M.; Williams, G. J. B. *J. Am. Chem. Soc.* **1981**, *103*, 5890–5893.
(6) Hanson, L. K.; Hofrichter, J. *Photochem. Photobiol.* **1985**, *41*, 247–249.
(7) Davydov, A. S. *Theory of Molecular Excitations*; McGraw-Hill: New York, 1962.
(8) Craig, D. P.; Walmsley, S. H. *Excitons in Molecular Crystals*; W. A. Benjamin: New York, 1968.

0002-7863/89/1511-4277$01.50/0

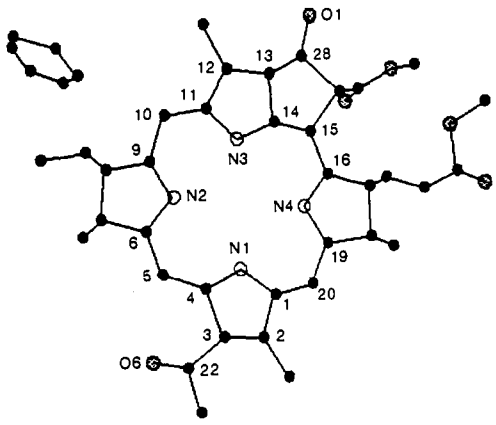

Figure 1. Structure of MeBPh. This is a planar projection of one unit cell of the crystal[5] in the mean plane of the N atoms. Atoms that are part of the π system are numbered as in ref 5. The benzene of crystallization in the same unit cell also is shown. Hydrogen atoms are not shown but are included in all of the calculations of electrostatic energies described in the text.

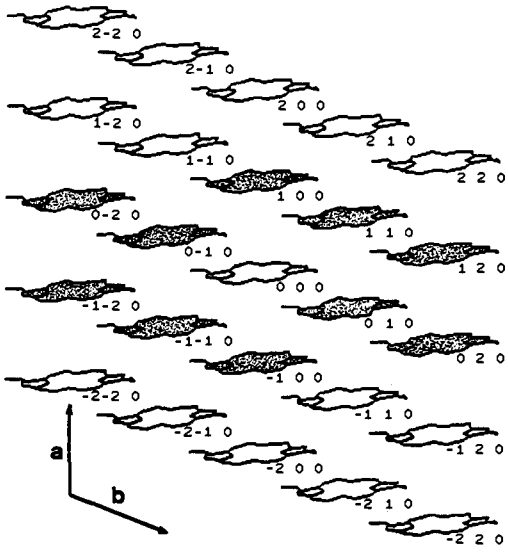

Figure 2. Planar projection of the molecules in a crystallographic **ab** plane of the MeBPh crystal.[5] The directions of the **a** and **b** axes are indicated; the **c** axis is approximately perpendicular to the **ab** plane. Crystallographic coordinates (r_a,r_b,r_c) of the molecules are indicated relative to a molecule at an arbitrary position (0,0,0). Only atoms that are part of the π system are shown. In each molecule, ring I and its attached acetyl group are to the right, and ring III and the keto group of ring V are to the left. The molecules that serve as electron acceptors in the CT transitions considered in Table IV and Figures 3 and 4 are shaded.

here consider this more general problem, following the same approach that we used for photosynthetic reaction centers.[1,2] Special emphasis is placed on evaluating the CT transition energies by using experimentally measured reduction potentials and direct microscopic calculations of electrostatic interactions, to reduce the problems associated with gas-phase calculations of molecular orbital energies. The treatment is restricted to the case of a crystal in which each unit cell has one spectroscopically active molecule, since the MeBPh crystal is of this type;[5] it could be extended straightforwardly to crystals with more than one molecule per unit cell.[7-9]

Interaction Matrix Elements for Excited States in a Crystal. The approach described in ref 1 starts by writing π molecular orbitals for an individual molecule of MeBPh as linear combinations of atomic orbitals:

$$\phi_n = \sum_t v_{n,t}\chi_t \tag{1}$$

where χ_t is an atomic p_z orbital on atom t. The expansion coefficients $v_{n,t}$ can be obtained conveniently by the semiempirical QCFF/PI method.[10] Because the spectroscopic properties of MeBPh and other molecules related to chlorophyll are due predominantly to excitations from the two highest filled molecular π orbitals to the two lowest unoccupied orbitals,[1,11] we shall focus our attention on these four orbitals. They will be designated as ϕ_1, ϕ_2, ϕ_3, and ϕ_4 in order of increasing energy.

Wave functions for the excited singlet states of an individual molecule (R) can be written as

$$^1\Psi^R{}_i = \sum_N c_{i,N}\,{}^1\Psi^R{}_N \tag{2}$$

where $^1\Psi^R{}_N$ is the singlet wave function corresponding to excitation from molecular orbital ϕ_{n1} to orbital ϕ_{n2}, and the coefficients $c_{i,N}$ are obtained by diagonalizing a configuration-interaction matrix. In the four-orbital model, this procedure gives four excited states, which are generally termed Q_y, Q_x, B_x, and B_y.[1,11] The Q_y, Q_x, B_x, and B_y transitions of an isolated molecule of MeBPh or bacteriopheophytin *a* in solution occur near 754, 530, 385, and 360 nm and have dipole strengths of approximately 39, 13, 37, and 80 D^2, respectively.[6,12] Using these wavelengths to fix the energies of the local transitions, one can adjust the coefficients in (2) so that the Q_y and Q_x dipole strengths calculated from the molecular orbitals agree with the experimental values.[1] This provides a useful basis for analyzing intermolecular interactions in a crystal.

An excited electronic state of a molecular crystal can be expressed similarly as a linear combination of excitations associated with the individual molecules:

$$^1\Psi_k = \sum_{\mathbf{R}}\sum_{\mathbf{r}}\sum_N C^{\mathbf{R},\mathbf{r}}{}_{k,N}\,{}^1\Psi^{\mathbf{R},\mathbf{r}}{}_N \tag{3}$$

where the wave function $^1\Psi^{\mathbf{R},\mathbf{r}}{}_N$ corresponds to a singlet excitation from molecular orbital ϕ_{n1} of molecule **R** to ϕ_{n2} of molecule **R′**, with $\mathbf{R}' = \mathbf{R} + \mathbf{r}$. **R** and **r** can be interpreted as vectors, $\mathbf{R} = R_a\mathbf{a} + R_b\mathbf{b} + R_c\mathbf{c}$ and $\mathbf{r} = r_a\mathbf{a} + r_b\mathbf{b} + r_c\mathbf{c}$, where the R_i and r_i are integers and the basis vectors **a**, **b**, and **c** form the edges of the crystal's unit cell. The **r** vector is (0,0,0) for an intramolecular excitation and nonzero for an intermolecular CT transition.

Equation 3 leads to a set of coupled equations for the coefficients $C^{\mathbf{R},\mathbf{r}}{}_{k,N}$ and transition energies ΔE_k of the crystal's excited states:

$$\sum_{\mathbf{R}}\sum_{\mathbf{r}}\sum_{N(\mathbf{R}\mathbf{r}N\neq\mathbf{S}\mathbf{s}M)} A_{\mathbf{R}\mathbf{r}N,\mathbf{S}\mathbf{s}M}C^{\mathbf{R},\mathbf{r}}{}_{k,N} + (\Delta E^{\mathbf{s}}{}_M - \Delta E_k)C^{\mathbf{S},\mathbf{s}}{}_{k,M} = 0 \tag{4}$$

Here $A_{\mathbf{R}\mathbf{r}N,\mathbf{S}\mathbf{s}M}$ is a configuration-interaction matrix element[1] that mixes $^1\Psi^{\mathbf{R},\mathbf{r}}{}_N$ and $^1\Psi^{\mathbf{S},\mathbf{s}}{}_M$. $\Delta E^{\mathbf{s}}{}_M$ is the energy of an individual excitation of type ($\mathbf{s}$,M), which will be independent of **S** if all of the spectroscopically active molecules in the crystal are identical. The subscript ($\mathbf{R}\mathbf{r}N \neq \mathbf{S}\mathbf{s}M$) means that terms for $N = M$ are excluded from the sum if and only if $\mathbf{R} = \mathbf{S}$ and $\mathbf{r} = \mathbf{s}$.

Because of the translational symmetry of the crystal, $C^{\mathbf{R},\mathbf{r}}{}_{k,N}$ can be expressed in the form

$$C^{\mathbf{R},\mathbf{r}}{}_{k,N} = C_{k,N}e^{i\mathbf{q}\cdot\mathbf{R}} \tag{5}$$

with

$$\mathbf{q} = 2\pi q_a\mathbf{a}^* + 2\pi q_b\mathbf{b}^* + 2\pi q_c\mathbf{c}^*$$

where q_a, q_b, and q_c are integers and $\mathbf{a}^*$, $\mathbf{b}^*$, and $\mathbf{c}^*$ are the vectors of the crystal's reciprocal lattice.[7,8] The reciprocal lattice vectors are given by $\mathbf{a}^* = \mathbf{b}\times\mathbf{c}/(\mathbf{a}\cdot\mathbf{b}\times\mathbf{c})$ and similarly for $\mathbf{b}^*$ and $\mathbf{c}^*$. Inserting eq 5 into eq 4 gives

(9) *Modern Quantum Chemistry Part III. Action of Light and Organic Crystals*; Sinonoglu, O., Ed.; Academic Press: New York, 1965.

(10) (a) Warshel, A.; Lappicerella, A. *J. Am. Chem. Soc.* **1981**, *103*, 4664-4673. (b) Warshel, A.; Levitt, M. *Quantum Chemistry Program Exchange*, No. 247; Indiana University, 1974.

(11) Gouterman, M. *J. Mol. Spectrosc.* **1961**, *6*, 138-163.

(12) Scherz, A.; Parson, W. W. *Biochim. Biophys. Acta* **1985**, *766*, 666-678.

$$\sum_{\mathbf{R}}\sum_{\mathbf{r}}\sum_{N}({}^{\mathbf{r}}N\neq{}^{\mathbf{s}}M)(A_{{}^{\mathbf{r}}N,{}^{\mathbf{s}}M}e^{i\mathbf{q}\cdot(\mathbf{R}-\mathbf{S})})C^{\mathbf{r}}_{k,N} + (\Delta E^{\mathbf{s}}_{M} - \Delta E_k)C^{\mathbf{s}}_{k,M} = 0 \quad (6)$$

or

$$\sum_{\mathbf{r}}\sum_{N}A'_{{}^{\mathbf{r}}N,{}^{\mathbf{s}}M}\,C^{\mathbf{r}}_{k,N} + (\Delta E^{\mathbf{s}}_{M} - \Delta E_k)C^{\mathbf{s}}_{k,M} = 0 \quad (7)$$

with

$$A'_{{}^{\mathbf{r}}N,{}^{\mathbf{s}}M} = \sum_{\mathbf{R}}({}^{\mathbf{r}}N\neq{}^{\mathbf{s}}M)A_{{}^{\mathbf{R}}{}^{\mathbf{r}}N,{}^{\mathbf{S}}{}^{\mathbf{s}}M}e^{i\mathbf{q}\cdot(\mathbf{R}-\mathbf{S})} \quad (8)$$

The coefficients $C^{\mathbf{r}}_{k,N}$ and transition energies for any particular value of the wave vector $\mathbf{q}$ are the eigenvectors and eigenvalues of the matrix equation

$$\mathbf{A''C} = \Delta E C \quad (9)$$

where $A''_{{}^{\mathbf{r}}N,{}^{\mathbf{s}}M} = \delta_{{}^{\mathbf{r}}N,{}^{\mathbf{s}}M}\,\Delta E^{\mathbf{r}}_{N} + A'_{{}^{\mathbf{r}}N,{}^{\mathbf{s}}M}$. It will suffice to consider only the solutions for $|\mathbf{q}| = 0$, because only these states have nonzero transition dipoles for optical excitation from the ground state.[7,8] The matrix elements of $\mathbf{A''}$ then simplify to

$$A''_{{}^{\mathbf{r}}N,{}^{\mathbf{s}}M} = \delta_{{}^{\mathbf{r}}N,{}^{\mathbf{s}}M}\Delta E^{\mathbf{r}}_{N} + \sum_{\mathbf{S}}({}^{\mathbf{S}}{}^{\mathbf{s}}M\neq{}^{\mathbf{R}}{}^{\mathbf{r}}N)A_{{}^{\mathbf{R}}{}^{\mathbf{r}}N,{}^{\mathbf{S}}{}^{\mathbf{s}}M} \quad (10)$$

Rather than diagonalizing $\mathbf{A''}$ directly, it is useful first to apply the intermediate transformation expressed by eq 2, so as to diagonalize the groups of intramolecular excitations that correspond to r or s = (0,0,0). As was discussed in ref 1 for the case of a dimer, this transformation converts $\mathbf{A''}$ into a new matrix $\mathbf{U}$, which can be arranged into three submatrices. One of the submatrices contains only exciton-type interactions of the intramolecular transitions; another submatrix contains only intermolecular CT transitions; and the third submatrix contains the interactions of local transitions with CT transitions. The effects of intermolecular orbital overlap appear mainly in the third, off-diagonal submatrix.[1]

The individual interaction terms $A_{{}^{\mathbf{R}}{}^{\mathbf{r}}N,{}^{\mathbf{S}}{}^{\mathbf{s}}M}$ that contribute to $\mathbf{U}$ can be evaluated by expanding the molecular orbitals as in eq 1 and using expressions given in ref 1. For the exciton-type interactions of two intramolecular transitions (transitions i and k with r and s = 0), this gives

$$U_{0i,0k} = \delta_{i,k}\Delta E^{0}_{i} + \sum_{\mathbf{S}\neq\mathbf{R}}\sum_{\mathbf{N}}\sum_{\mathbf{M}}c_{i,N}c_{k,M}A_{{}^{\mathbf{R}}{}^{\mathbf{r}}N,{}^{\mathbf{S}}{}^{\mathbf{s}}M} = \delta_{i,k}\Delta E^{0}_{i} + \sum_{\mathbf{S}\neq\mathbf{R}}U^{\mathrm{ex}}\mathbf{R}i,\mathbf{S}k \quad (11)$$

$$= \delta_{i,k}\Delta E^{0}_{i} + \sum_{\mathbf{S}\neq\mathbf{R}}\Omega_{i,k}\sum_{\mathbf{N}}\sum_{\mathbf{M}}c_{i,N}c_{k,M}(2\sum_{t_R}\sum_{t_S}\upsilon_{n1,t_R}\upsilon_{n2,t_R}\upsilon_{m1,t_S}\upsilon_{m2,t_S}\gamma_{t_R,t_S}) \quad (12)$$

where ΔE^{0}_{i} is the energy of an intramolecular transition of type i, γ_{t_R,t_S} is the electron–electron repulsion integral between atomic p_z orbitals on atom t_R of molecule $\mathbf{R}$ and atom t_S of molecule $\mathbf{S}$, and $\Omega_{i,k}$ is a factor that corrects for the tendency of the π molecular orbital treatment to overestimate transition dipole magnitudes.[1] Equation 11 differs from the corresponding eq 23 of ref 1 in that the exciton interactions of transitions i and k for all of the molecules in the crystal are collected in a sum over $\mathbf{S}$. A sum of this type contributes to each of the diagonal matrix elements $U_{0i,0i}$, as well as to the off-diagonal elements.

In the four-orbital model, a given pair of molecules ($\mathbf{R}$ and $\mathbf{R}'$) can enter into four main CT transitions ($^{1}\Psi^{\mathbf{R},\mathbf{r}}{}_{N}$), in which an electron moves from orbital ϕ_1 or ϕ_2 of $\mathbf{R}$ to either ϕ_3 or ϕ_4 of $\mathbf{R}'$ [N = (ϕ_2,ϕ_3), (ϕ_2,ϕ_4), (ϕ_1,ϕ_3), or (ϕ_1,ϕ_4)]. These CT transitions are not diagonalized by the intermediate transformation of $\mathbf{A''}$ into $\mathbf{U}$. They contribute separate interaction matrix elements of the form

$$U_{{}^{\mathbf{r}}N,{}^{\mathbf{r}}M} = \delta_{N,M}\Delta E^{\mathbf{r}}_{N} - (1 - \delta_{N,M})\sum_{t_R}\sum_{t_{R'}}\upsilon_{n1,t_R}\upsilon_{m1,t_R}\upsilon_{n2,t_{R'}}\upsilon_{m2,t_{R'}}\gamma_{t_R,t_{R'}} \quad (13)$$

where $\Delta E^{\mathbf{r}}_{N}$ is the energy of a CT basis transition of type ($\mathbf{r}$,N). $\mathbf{U}$ includes a set of four matrix elements of this type for each value of the intermolecular vector $\mathbf{r}$. However, the CT excitations acquire dipole strength only by the mixing with the intramolecular transitions, and this mixing falls off rapidly with $|\mathbf{r}|$. One therefore needs to consider only a restricted set of CT transitions involving molecules that are relatively close together. This point will be explored below for the specific case of the MeBPh crystal. CT transitions in which $\mathbf{R}$ serves as an electron acceptor instead of a donor do not need to be listed separately; they are included automatically by taking the sums in eq 3 over all $\mathbf{R}$ and r.

Note that the sum over $\mathbf{S}$ that appears in eq 10 collapses into a single term for $\mathbf{S} = \mathbf{R}$ in eq 13. Charge-transfer transitions of a pair of molecules in a given spatial relationship ($^{1}\Psi^{\mathbf{R},\mathbf{r}}{}_{N}$) do not interact significantly with the CT transitions of any other pair with the same spatial relationship ($^{1}\Psi^{\mathbf{S},\mathbf{r}}{}_{M}$ with $\mathbf{S} \neq \mathbf{R}$). In this case, eq 15 of ref 1 evaluates to zero because the two electron donors or acceptors must always be different molecules with no atomic p_z orbitals in common. The diagonal matrix elements for CT transitions are therefore essentially equal to the individual CT transition energies, $\Delta E^{\mathbf{r}}_{N}$. The factor $(1 - \delta_{N,M})$ in eq 13 specifies that we omit the sum of electron repulsion integrals for the diagonal matrix elements ($\delta_{N,M} = 1$), which means that the electrostatic interactions between the two radicals must be included in $\Delta E^{\mathbf{r}}_{N}$. The evaluation of these energies is discussed in more detail below.

For the interaction of an intramolecular excitation of type k with a CT transition of type ($\mathbf{r}$,N), the matrix elements of $\mathbf{U}$ evaluate to

$$U_{0k,{}^{\mathbf{r}}N} = \sum_{\mathbf{S}}\sum_{\mathbf{M}}c_{k,M}(\delta_{R,S}\delta_{n1,m1}\sum_{t_{R'}}\sum_{t_S}\upsilon_{n2,t_{R'}}\upsilon_{m2,t_S}\beta_{t_{R'},t_S} - \delta_{R',S}\delta_{n2,m2}\sum_{t_R}\sum_{t_S}\upsilon_{n1,t_R}\upsilon_{m1,t_S}\beta_{t_R,t_S}) = \sum_{\mathbf{M}}c_{k,M}\sum_{t_R}\sum_{t_{R'}}(\delta_{n1,m1}\upsilon_{n2,t_{R'}}\upsilon_{m2,t_R} - \delta_{n2,m2}\upsilon_{n1,t_R}\upsilon_{m1,t_{R'}})\beta_{t_R,t_{R'}} \quad (14)$$

where $\beta_{a,b}$ is the resonance integral for p_z orbitals on atoms a and b, and indices t_R, $t_{R'}$, and t_S refer to atoms on molecules $\mathbf{R}$, $\mathbf{R}'$, and $\mathbf{S}$, respectively. When the two transitions start from the same molecular orbital ($\delta_{R,S}\delta_{n1,m1} = 1$), the atomic resonance integrals are summed over the two final orbitals; when the transitions end in the same molecular orbital ($\delta_{R',S}\delta_{n2,m2} = 1$), the sum is taken over the two initial orbitals. Like eq 11, this expression differs from the corresponding eq 27 and 28 of ref 1 by the inclusion of a sum over $\mathbf{S}$. In this case, however, the sum collapses to two terms, one for $\mathbf{S} = \mathbf{R}$ and one for $\mathbf{S} = \mathbf{R}'$.

Pairs of CT transitions involving two different intermolecular vectors (r and s) have interaction matrix elements of the form

$$U_{{}^{\mathbf{r}}N,{}^{\mathbf{s}}M} = \delta_{n1,m1}\sum_{t_{R'}}\sum_{t_{R'(s)}}\upsilon_{n2,t_{R'}}\upsilon_{m2,t_{R'(s)}}\beta_{t_{R'},t_{R'(s)}} \quad (15)$$

Here $t_{R'}$ and $t_{R'(s)}$ refer to atoms on molecules ($\mathbf{R} + \mathbf{r}$) and ($\mathbf{R} + \mathbf{s}$), respectively. In this case, the sum over $\mathbf{S}$ consists of only the single term in which $\mathbf{S} = \mathbf{R}$.

Semiempirical expressions for the atomic repulsion and resonance integrals $\gamma_{a,b}$ and $\beta_{a,b}$ have been given in ref 1.

Evaluation of Matrix Elements for the MeBPh Crystal. MeBPh crystallizes in the triclinic $P\bar{1}$ space group with unit cell edge lengths $|\mathbf{a}| = 7.25$ Å, $|\mathbf{b}| = 8.11$ Å, and $|\mathbf{c}| = 17.22$ Å.[5] The arrangement of the molecules in the crystallographic **ab** planes is shown in Figure 2.

The principal components of the diagonal matrix elements $U_{0i,0i}$ in eq 11 are the energies of the intramolecular excitations, ΔE^{0}_{i}. These can be expressed as

$$\Delta E^{0}_{i} = \Delta E^{\mathrm{w}}_{i} + [\Delta E^{0}_{i,\mathrm{disp}} + \Delta E^{0}_{i,\mathrm{elec}} - \Delta E^{\mathrm{w}}_{i,\mathrm{disp}} - \Delta E^{\mathrm{w}}_{i,\mathrm{elec}}] \quad (16)$$

Here $\Delta E^{\mathrm{w}}_{i}$ is the energy of the spectroscopic transition of monomeric MeBPh in solution; $\Delta E^{0}_{i,\mathrm{elec}}$ represents the change in electrostatic interactions of the excited molecule with the surrounding molecules in the crystal (relative to the electrostatic interaction energy of the unexcited molecule); and $\Delta E^{\mathrm{w}}_{i,\mathrm{elec}}$ represents the corresponding change in electrostatic interactions for the molecule in solution. $\Delta E^{0}_{i,\mathrm{disp}}$ and $\Delta E^{\mathrm{w}}_{i,\mathrm{disp}}$ represent "dispersion" effects that are not included in eq 11. The dispersion terms arise from mixing of the excited state with states in which two molecules are excited simultaneously, and from mixing of the ground state with the doubly excited states and with CT states.

Table I. Exciton Interaction Energies in Crystalline MeBPh[a]

r_{max}, Å	molecules[b]	$\sum_{S\neq R} U^{ex}_{R_i,S_j}$, cm^{-1}			
		Q_y	Q_x	B_x	B_y
10	6	−369	869	6146	−737
15	12	−189	1026	7366	−486
20	36	−564	921	6278	−1000
25	72	−633	844	5648	−1106
30	120	−665	858	5789	−1152
35	176	−696	881	5950	−1204
40	290	−680	852	5723	−1176
45	410	−677	857	5762	−1172
50	542	−700	870	5869	−1207
55	740	−669	862	5805	−1159

[a] Summed interaction energies for pairs of intramolecular transitions of the same type (Q_y, Q_x, B_x, B_y), calculated with eq 11 and 12. The calculations consider all of the MeBPh molecules within a sphere of radius r_{max} around a fixed molecule at $\mathbf{r}$ = (0,0,0). Table II includes interaction energies for transitions of different types. [b] Number of MeBPh molecules with centers inside the sphere (not counting the central molecule).

For the molecule in solution, the dispersion effects involve interactions with excited states of the solvent.

With MeBPh in CH_2Cl_2–benzene, the energies of the Franck–Condon absorption maxima are approximately 13 260 cm^{-1} for the Q_y transition, 18 670 for Q_x, 25 970 for B_x, and 28 170 for B_y.[6] It should be acceptable to use these values for the ΔE^w_i, rather than attempting to estimate the 0–0 transition energies, because the intramolecular vibronic couplings are probably not very different in the crystal and in solution.

The sums of the electrostatic and dispersion energy differences that are collected in brackets in eq 16 could cause shifts on the order of ±100 cm^{-1} in the ΔE^w_i. The absorption maxima of MeBPh in solution are not expected to be very sensitive to the solvent, because the ground state and the $\pi\pi^*$ excited states are all relatively nonpolar. In nine different solvents (acetone, acetonitrile, benzene, CCl_3, CCl_4, dimethyl sulfoxide, ethanol, ethyl acetate, and pyridine), the position of the Q_y band of bacteriopheophytin a varies from 746 to 758 nm, a range of 212 cm^{-1}, and the Q_x band varies from 525 to 532 nm (251 cm^{-1}) [W. Parson, O. Oleinik, and M. Becker, unpublished results]. Similar results have been obtained by Callahan and Cotton.[13] The energies quoted above for MeBPh in CH_2Cl_2–benzene[6] fall in the centers of these ranges. Although one can write analytical expressions for the dispersion and electrostatic energies associated with intramolecular transitions in the crystal, calculations of these relatively small terms are probably not very reliable. The results depend on the details of the molecular orbitals much more than do calculations of electrostatic effects on intermolecular CT transitions, and corrections based on experimental measurements are not well grounded. We shall, therefore, neglect these terms here, and discuss them in more detail elsewhere. (The calculations described below do include the small contributions of doubly excited states to the transition double strengths. These were treated essentially as described previously for smaller oligomers.[1,12])

To analyze the exciton-type interactions of intramolecular transitions in the MeBPh crystal, we calculated the sums in eq 12 over all of the molecules (**S**) centered within a sphere with a given radius r_{max} around the fixed molecule **R**. Table I lists the values of the sums that contribute to the diagonal matrix elements $U_{0i,0i}$. Results are shown for a range of values of r_{max}, with the total number of neighboring molecules varying from 6 to 740. The sums become relatively insensitive to the size of the sphere once the radius is greater than about 30 Å. All of the results presented below are based on calculations with r_{max} = 55 Å. For the Q_y transition, the summed exciton interactions amount to −670 cm^{-1}, which would account for about 40% of the red shift of 1675 cm^{-1} that is found experimentally.[6]

Combining the exciton interaction energies with the intramolecular transition energies gives values of approximately 12 590, 19 530, 31 770 and 26 540 cm^{-1} for the Q_y, Q_x, B_x, and B_y diagonal matrix elements, respectively. Note that this reverses the order of the B_x and B_y transitions. These energies are collected in Table II, along with the off-diagonal matrix elements for the intramolecular transitions, as obtained by using eq 12. Table II also lists some of the matrix elements involving CT transitions, which we take up next.

Each molecule of MeBPh in the crystal can participate directly in CT transitions with four neighboring molecules in the same crystallographic **ab** plane (Figure 2). In the four-orbital model, this gives 16 principal types of CT transitions, which interact with the intramolecular transitions as described by eq 14. Charge-transfer transitions in the **c** direction are unimportant because of the larger dimension of the unit cell in this direction. In addition to the 16 principal CT transitions, there is a hierarchy of transitions in which electrons move from molecule **R** to more distant molecules in the same **ab** plane. These transitions do not interact directly with the intramolecular transitions of either **R** or the electron acceptor (**R′**) to any significant extent, because of the rapid decay of the resonance integrals with distance. But they do mix with other CT transitions as described by eq 15, and this mixing connects them indirectly to the intramolecular transitions. For example, a CT transition in which an electron moves from **R** at (0,0,0) to the neighbor at (0,1,0) can interact with the transitions in which the electron moves from the same orbital of **R** to one of the three more distant neighbors at (0,2,0), (1,2,0), and (−1,0,0).

Table II includes the matrix elements for the interactions of the four types of intramolecular transitions with the CT transitions involving the 10 nearest neighbors in the **ab** plane, as calculated with eq 14. The Q_y transitions interact particularly strongly with CT transitions involving the four molecules at (0,1,0), (0,−1,0), (1,1,0), and (−1,−1,0). To illustrate higher order interactions, the table also lists the matrix elements that interconnect the four different CT transitions for $\mathbf{r}$ = (0,1,0), as calculated by using eq 13, and the matrix elements that couple these transitions to CT transitions with some other values of r (eq 15). The interactions of CT transitions with different values of **r** are strong when one of the two electron donors or acceptors is among the four nearest neighbors of the other but are negligible when the molecules are farther apart. The diagonal CT transition energies given in Table II are discussed in the following section.

Electrostatic Energies of CT Transitions in a Crystal. The diagonal energies of the CT transitions in crystalline MeBPh cannot be measured directly, and their calculation is not entirely straightforward. In general, the energy of a CT transition in which an electron moves from orbital ϕ_{n1} of molecule **R** to orbital ϕ_{n2} of **R′** is

$$\Delta E^{\tau}_N = \alpha_N + \Delta E^{\tau}_{elec} \qquad (17)$$

Here α_N is the difference between the gas-phase energies of the two orbitals ($E_{n2} - E_{n1}$) when the two molecules are infinitely far apart, and ΔE^{τ}_{elec} is the total energy of electrostatic interactions of the two charged species $\mathbf{R}^+$ and $\mathbf{R}'^-$ with each other and with their surroundings when the molecules are separated by a finite distance in the crystal (relative to the corresponding energy for the neutral species). Equation 17 neglects the stabilization of the ground state by dispersion effects, as did our treatment of the intramolecular transition energies.

An initial estimate of the orbital energy difference α_N can be obtained from the QCFF/PI molecular orbital calculations. For the lowest energy CT transition, in which an electron moves from orbital ϕ_2 of molecule **R** to ϕ_3 of **R′**, α_N is calculated to be approximately 33 000 cm^{-1}. The three higher CT transitions of the same donor and acceptor are calculated to lie above this one by approximately 11 600 cm^{-1} for N = (ϕ_2,ϕ_4), 19 200 cm^{-1} for (ϕ_1,ϕ_3), and 30 800 cm^{-1} for (ϕ_1,ϕ_4).

The size and complexity of MeBPh make such quantum mechanical calculations of α_N subject to considerable uncertainty. We have therefore explored an alternative approach[14] that makes

(13) Callahan, P. M.; Cotton, T. M. *J. Am. Chem. Soc.* **1987**, *109*, 7001–7007.

(14) Creighton, S.; Hwang, J.-K.; Warshel, A.; Parson, W. W.; Norris, J. *Biochemistry* **1988**, *27*, 774–781.

Table II. Representative Matrix Elements of **U** (in cm^{-1})

	intramolecular transitions				CT transitions, **r** = (0,1,0)			
	Q_y	Q_x	B_x	B_y	(ϕ_2,ϕ_3)	(ϕ_2,ϕ_4)	(ϕ_1,ϕ_3)	(ϕ_1,ϕ_4)
Q_y	12590	279	663	−890	−1457	42	−47	72
Q_x	279	19530	2256	214	22	−282	359	−66
B_x	663	2256	31770	473	141	−151	−671	−11
B_y	−890	214	473	26540	−268	−107	−96	−394
r = (0,1,0)								
(ϕ_2,ϕ_3)	−1457	22	141	−268	17000	211	−369	12
(ϕ_2,ϕ_4)	42	−282	−151	−107	211	28600	12	−362
(ϕ_1,ϕ_3)	−47	359	−671	−96	−369	12	36200	213
(ϕ_1,ϕ_4)	72	−66	−11	−394	12	−362	213	47800
r = (0,−1,0)								
(ϕ_2,ϕ_3)	−1457	49	−47	−268	0	0	0	0
(ϕ_2,ϕ_4)	73	−282	−151	78	0	0	0	0
(ϕ_1,ϕ_3)	115	359	−671	−1	0	0	0	0
(ϕ_1,ϕ_4)	72	59	129	−394	0	0	0	0
r = (1,1,0)								
(ϕ_2,ϕ_3)	508	−231	−84	93	0.13	0	0.19	0
(ϕ_2,ϕ_4)	−291	225	120	−89	0	0.13	0	0.19
(ϕ_1,ϕ_3)	141	−8	14	273	0.31	0	−0.04	0
(ϕ_1,ϕ_4)	−44	309	−178	241	0	0.31	0	−0.04
r = (−1,−1,0)								
(ϕ_2,ϕ_3)	508	−356	23	93	0	0	0	0
(ϕ_2,ϕ_4)	−205	225	120	−228	0	0	0	30
(ϕ_1,ϕ_3)	−20	−8	14	305	0	0	0	0
(ϕ_1,ϕ_4)	−44	146	−198	241	0	0	0	0
r = (1,0,0)								
(ϕ_2,ϕ_3)	−0.24	−0.25	0.22	−0.04	0	0	0	0
(ϕ_2,ϕ_4)	−0.15	0.53	0.28	−0.34	0	0	0	0
(ϕ_1,ϕ_3)	0.16	0.20	−0.37	0.15	0	0	0	0
(ϕ_1,ϕ_4)	0.08	0.27	−0.10	−0.42	0	0	0	0
r = (−1,0,0)								
(ϕ_2,ϕ_3)	−0.24	−0.28	0.07	−0.04	331	0	35	0
(ϕ_2,ϕ_4)	−0.08	0.53	0.28	−0.21	0	331	0	35
(ϕ_1,ϕ_3)	0.26	0.20	−0.37	0.27	188	0	−169	0
(ϕ_1,ϕ_4)	0.08	0.32	0.04	−0.42	0	188	0	−169
r = (1,2,0)								
(ϕ_2,ϕ_3)	−0.068	0.026	−0.017	−0.013	331	0	188	0
(ϕ_2,ϕ_4)	−0.020	−0.031	−0.017	0.024	0	331	0	188
(ϕ_1,ϕ_3)	0.018	0.020	−0.037	−0.012	35	0	−169	0
(ϕ_1,ϕ_4)	−0.013	0.021	−0.006	0.007	0	35	0	−169
r = (−1,−2,0)								
(ϕ_2,ϕ_3)	−0.068	−0.021	0.007	−0.013	0	0	0	0
(ϕ_2,ϕ_4)	0.017	−0.031	−0.017	−0.013	0	0	0	0
(ϕ_1,ϕ_3)	−0.029	0.020	−0.037	0.010	0	0	0	0
(ϕ_1,ϕ_4)	−0.013	−0.031	0.000	0.007	0	0	0	0
r = (0,2,0)								
(ϕ_2,ϕ_3)	0.0020	−0.0015	0.0009	0.0004	−653	0	−64	0
(ϕ_2,ϕ_4)	0.0011	0.0005	0.0027	−0.0014	0	−654	0	−64
(ϕ_1,ϕ_3)	−0.0011	−0.0006	0.0011	−0.0007	113	0	67	0
(ϕ_1,ϕ_4)	−0.0000	0.0012	−0.0003	−0.0003	0	113	0	67
r = (0,−2,0)								
(ϕ_2,ϕ_3)	0.0020	−0.0011	−0.0005	−0.0004	0	0	0	0
(ϕ_2,ϕ_4)	−0.0011	0.0005	0.0027	0.0008	0	0	0	0
(ϕ_1,ϕ_3)	−0.0017	−0.0006	0.0011	−0.0005	0	0	0	0
(ϕ_1,ϕ_4)	−0.0000	0.0018	−0.0001	0.0003	0	0	0	0

use of experimentally measured electrochemical reduction potentials for the formation of the $MeBPh^+$ and $MeBPh^-$ radicals separately in solution:

$$\alpha_N = \Delta G^w(\infty) - \Delta G^w{}_{sol} \qquad (18)$$

Here $\Delta G^w(\infty)$ is the free energy change obtained by subtracting the two reduction potentials, and $\Delta G^w{}_{sol}$ is the sum of the calculated free energies of solvation of the two radicals (at infinite distance from each other) by a polar solvent, again relative to the calculated solvation energy of the neutral molecules. This expression pertains to the lowest energy CT transition, $N = (\phi_2,\phi_3)$. Although the reduction potentials for MeBPh itself have not be reported, values for bacteriopheophytin a (BPh) are known[15] and should be very similar. The midpoint potential for the BPh^+/BPh half-reaction is +0.96 V with respect to the H^+/H_2 half-cell; that for BPh/BPh^- is −0.55 V. Combining these values gives $\Delta G^w(\infty)$ = 1.51 eV, or 34.8 kcal/mol.

$\Delta G^w{}_{sol}$ can be estimated in several different ways.[16-19] Probably the most reliable is a free energy perturbation method involving an adiabatic charging of the radical.[18,19] To implement these calculations, we used the surface-constrained all-atoms solvent (SCAAS) model[17,18] with 100 molecules of water in the explicit solvent region, including 35 molecules in the surface-constrained region. The constraints ensure that the polarization of the surface molecules is close to that expected for an infinite system. The solvent outside the surface region was treated as a continuum with

(15) Fajer, J.; Davis, M. S.; Brune, D. C.; Spaulding, L. D.; Borg, D. C.; Forman, A. *Brookhaven Symp. Biol.* **1976**, *28*, 74–103.

(16) Russell, S. T.; Warshel, A. *J. Mol. Biol.* **1985**, *185*, 389–404.
(17) Warshel, A.; Russell, S. T. *Q. Rev. Biophys.* **1984**, *17*, 283–422.
(18) Warshel, A.; Sussman, F.; King, G. *Biochemistry* **1986**, *25*, 8368–8372.
(19) Warshel, A. *J. Phys. Chem.* **1982**, *86*, 2218–2224.

Table III. Partial Charges[a] of π Atoms in Neutral, Oxidized, and Reduced MeBPh

atom[b]	MeBPh	$MeBPh^+$	$MeBPh^-$
C1	0.122	0.233	0.040
C2	−0.024	0.011	−0.082
C3	−0.004	0.037	−0.056
C4	0.120	0.236	0.045
C5	0.004	0.004	−0.030
C6	0.034	0.134	−0.027
C8	0.024	0.131	−0.046
C10	0.005	0.005	−0.025
C11	0.106	0.228	0.023
C12	−0.007	0.031	−0.067
C13	−0.008	0.025	−0.050
C14	0.126	0.235	0.052
C15	−0.029	−0.029	−0.049
C16	0.028	0.113	−0.025
C19	0.037	0.121	−0.021
C20	−0.021	−0.021	−0.044
C22	0.272	0.272	0.265
C28	0.267	0.267	0.262
N1	−0.449	−0.449	−0.449
N2	0.269	−0.269	0.221
N3	−0.446	−0.446	−0.446
N4	0.247	0.247	0.209
O1	−0.334	−0.325	−0.346
O2	−0.339	−0.329	−0.354

[a] These charges were obtained by the full QCFF/PI program.[10a] Similar results can be obtained using the Quantum Chemistry Program Exchange version of the program,[10b] with the simplified parameter set listed in Warshel and Lappicirella's[10a] Table IV. [b] Atoms are numbered as in Fig. 1.

a dielectric constant of 80. The adiabatic charging procedure employed the mapping potential

$$V_m = (1 - \lambda_m)V_1(\mathbf{Q}_1) + \lambda_m V_2(\mathbf{Q}_2) \quad (19)$$

Here $\mathbf{Q}_1$ and $\mathbf{Q}_2$ are the charge distributions in the neutral and ionic molecules; $V_1(\mathbf{Q}_1)$ and $V_2(\mathbf{Q}_2)$ are the solute–solvent interaction potentials for the neutral and ionic molecules, as represented by standard van der Waals and Coulombic terms; and λ_m is a mapping parameter that is increased gradually from 0 to 1 to drive the system from the neutral to the ionic charge distribution.[18,19] The corresponding free energies were obtained from the expressions

$$\Delta G_{1\rightarrow 2} = \sum \delta G(\lambda_m \rightarrow \lambda_{m'}) \quad (20)$$

$$\delta G(\lambda_m \rightarrow \lambda_{m'}) = -(k_B T) \ln \{\langle \exp(-[V_{m'} - V_m]/k_B T)\rangle_m\} \quad (21)$$

where $\langle\ \rangle_m$ represents an average calculated on potential energy surface V_m.[18,20]

The charge distributions $\mathbf{Q}_1$ and $\mathbf{Q}_2$ in eq 19 include the partial charge on each atom of the neutral MeBPh molecule ($\mathbf{Q}_1$) and of the $MeBPh^+$ or $MeBPh^-$ radical ($\mathbf{Q}_2$). However, the charges on atoms that are part of the π system are the most important, because only these change significantly when the molecule is oxidized or reduced. These charges can be obtained by the QCFF/PI treatment that is used for the molecular orbitals;[10] they are listed here in Table III.

The value of ΔG^w_{sol} obtained in this way was −76.8 kcal/mol, of which −39.8 kcal/mol was due to the radical cation and −37.0 kcal/mol to the anion. Combining ΔG^w_{sol} with $\Delta G^w(\infty)$ as in eq 18 gives $\alpha_{\phi 2,\phi 3}$ = 114.0 kcal/mol (38 600 cm^{-1}). The estimated uncertainty in this value is ±1800 cm^{-1}.

We also calculated ΔG^w_{sol} by the protein dipoles Langevin dipoles (PDLD) method,[16,17] in which a grid of Langevin dipoles is used to model the effects of solvent dipoles in a spherical region surrounding the radicals. This gave ΔG^w_{sol} = −83 kcal/mol (−44 kcal/mol for $MeBPh^+$ and −39 for $MeBPh^-$), leading to a somewhat higher value of $\alpha_{\phi 2,\phi 3}$ (41 000 cm^{-1}). However, the Langevin treatment of the solvated radical involves van der Waals parameters for the closest contact between the Langevin dipoles (the water molecules) and the solute atoms, and these parameters have not been calibrated for the present case of a π radical, in which the charges are located primarily on carbon atoms. The estimate of $\alpha_{\phi 2,\phi 3}$ obtained by this method is therefore less reliable than the estimate obtained by the adiabatic charging procedure.

With a reasonable estimate of $\alpha_{\phi 2,\phi 3}$, we can turn to the second term on the right-hand side of eq 17. This term, which represents the change in electrostatic interaction energy associated with the formation of a CT state in the crystal, is given by

$$\Delta E^r_{elec} = \Delta V^r_{QQ} + \Delta V^r_{Q\mu} + \Delta V^r_{ind} + \Delta V^r_{bulk} \quad (22)$$

Hee ΔV^r_{QQ} is the change in vacuum Coulombic interaction between the two radicals (molecules **R** and **R**′); $\Delta V^r_{Q\mu}$ is the change in the Coulombic interactions of molecules **R** and **R**′ with the permanent atomic charges on the surrounding molecules; ΔV^r_{ind} is the energy change associated with dipoles that **R** and **R**′ induce in the surrounding molecules; and ΔV^r_{bulk} represents the effects due to the bulk material outside the region in which $\Delta V^r_{Q\mu}$ and ΔV^r_{ind} are treated microscopically.[16,17]

ΔV^r_{QQ} is given by

$$V^r_{QQ} = -332 \text{ (kcal/mol)} \sum_{t_R} \sum_{t_{R'}} Q_{t_R} Q_{t_{R'}} / r_{t_R t_{R'}} \quad (23)$$

where Q_{t_R} and $Q_{t_{R'}}$ are the partial charges on atoms t_R of molecule **R** and $t_{R'}$ of molecule **R**′, and $r_{t_R t_{R'}}$ is the distance between these atoms. Similarly

$$V^r_{Q\mu} = -332 \text{ (kcal/mol)} \sum_{t_R} \sum_{t_S} Q_{t_R} Q_{t_S} / r_{t_R t_S} \quad (24)$$

where the first sum is taken over the atoms of both **R** and **R**′, and the second sum over the atoms of the neighboring molecules. A dielectric constant of 1 is used in the calculations of ΔV^r_{QQ} and $V^r_{Q\mu}$, since the dielectric effects of the neighboring molecules are included explicitly in ΔV^r_{ind}. In addition to the partial charges on the π atoms (Table III), these calculations included the charges on the two ester groups; a charge of +0.3 was used for an ester carbon, −0.25 for its carbonyl O, and −0.05 for the alcohol O.

The region for the calculation of $\Delta V^r_{Q\mu}$ and ΔV^r_{ind} was defined to include all of the atoms in each unit cell in which the MeBPh molecule was centered within a specified radius of the center of either the electron donor (**R**) or acceptor (**R**′). (As shown in Figure 1, each unit cell contains one molecule of MeBPh and one molecule of benzene of crystallization.[5]) Including entire unit cells in blocks ensures overall electrical neutrality. The cutoff radius for the molecular centers was set between 19.5 and 21 Å, depending on the position of the electron acceptor, so that the entire region contained between 5000 and 5500 atoms and 51–57 molecules of MeBPh. Varying the cutoff radius to change the number of atoms by 10–15% did not affect the results significantly. (The change in $|\Delta E^r_{elec}|$ was <0.2 kcal/mol.)

For most of the calculations, ΔV^r_{ind} was obtained from the expression

$$V^r_{ind} = -166 \text{ (kcal/mol)} \sum_{t_S} \rho_{t_S} (\xi_{t_S})^2 / d \quad (25)$$

where ξ_{t_S} is the vacuum field (in atomic charges/Å^2) on atom t_s in the region surrounding the radical pair, ρ_{t_S} is the atomic polarizability (in Å^3) of atom t_s, and d is an effective screening factor.[16] The field at each atom is obtained by summing the contributions from all of the other atoms in the system. A polarizability of 1.0 Å^3 was used for C, N, and O atoms, and 0.5 for H. A value of 1.11 was obtained for d by using the iterative, self-consistent-field expressions (6) and (8) of ref 16 with a smaller cutoff radius to define the region around the radical pair. (The iterative procedure becomes computationally impracticable when the region of interest contains more than about 2500 atoms.)

Finally, ΔV^r_{bulk} can be approximated by the Onsager expression

$$V^r_{bulk} = -166 \text{ (kcal/mol)}[2(\epsilon_0 - 1)/(2\epsilon_0 + 1)]|\mu|^2/b^3 \quad (26)$$

Here μ is the calculated dipole moment of the CT or ground state (in Å electron charge); b is the radius of the region that is included

(20) Valleau, J. P.; Torrie, G. M. In *Modern Theoretical Chemistry*; Berne, B. J., Ed.; Plenum: New York, 1977; Vol. 5, pp 169–194.

Table IV. Electrostatic Energies for CT Transitions in Crystalline MeBPh[a]

r (r_a,r_b,r_c)[b]	ΔV^{r}_{QQ}	$\Delta V^{r}_{Q\mu}$	ΔV^{r}_{ind}	ΔV^{r}_{bulk}	ΔG^{r}_{elec}	$\Delta E^{r}_{\phi 2,\phi 3}$
(0,1,0)	−43.9	−0.7	−15.0	−0.6	−60.2	17 400 (17 000)
0,−1,0)	−42.3	0.3	−15.2	−0.6	−57.8	18 300 (17 900)
(1,1,0)	−42.6	−1.9	−16.9	−0.6	−61.9	16 800 (16 400)
(−1,−1,0)	−38.2	1.5	−17.4	−0.8	−54.9	19 200 (18 800)
(1,0,0)	−41.6	−0.6	−22.1	−0.4	−64.7	15 800 (15 400)
(−1,0,0)	−36.8	−0.1	−22.9	−0.6	−60.4	17 400 (17 000)
(1,2,0)	−24.2	−3.8	−32.0	−1.4	−61.3	17 100 (16 700)
(−1,−2,0)	−21.5	3.1	−32.9	−1.6	−52.8	20 000 (19 600)
(0,2,0)	−21.5	−2.2	−35.1	−1.6	−60.4	17 300 (16 900)
(0,−2,0)	−20.5	1.6	−35.0	−1.6	−55.5	19 100 (18 700)

[a] Energies are in kcal/mol except for $\Delta E^{r}_{\phi 2,\phi 3}$, which is in cm^{-1}. For definitions of the terms, see text (eq 17–26). $\Delta E^{r}_{\phi 2,\phi 3}$ is obtained from ΔG^{r}_{elec} by eq 17, with $\alpha_{\phi 2,\phi 3}$ = 38 600 cm^{-1}. The values in parentheses are the CT transition energies obtained with $\alpha_{\phi 2,\phi 3}$ = 38 200 cm^{-1}, which bring the long-wavelength absorption band into agreement with the experimental observations (Figures 3 and 4). [b] Location of the electron acceptor, in crystallographic lattice steps relative to a donor at (0,0,0).

in detail (Å); and ϵ_0, the bulk (high-frequency) dielectric constant of the crystal, is taken to be 2.0 (see eq 45 of ref 17). Since the region that we treated microscopically was not strictly spherical, an effective value of b was obtained by calculating the density of the structure in spherical shells around the geometric center of the radical pair and taking the radius at which the density decreased to half of the crystal's bulk density of 1.23 g/cm^3. This was typically between 20 and 22 Å, depending on the location of the electron acceptor. A more complicated treatment of ΔV^{r}_{bulk} seems unnecessary, because this term makes a relatively minor contribution to ΔE_{elec}.

Table IV gives the calculated values of ΔV^{r}_{QQ}, $\Delta V^{r}_{Q\mu}$, ΔV^{r}_{ind}, ΔV^{r}_{bulk}, and ΔE^{r}_{elec} for the lowest energy CT transitions of a molecule in the crystal with its 10 nearest neighbors. To obtain the diagonal matrix elements for the CT transitions, ΔE^{r}_{elec} must be added to α_N (eq 17). Taking the estimate of α_N obtained by the adiabatic-charging procedure (38 600 tu 1800 cm^{-1}), one gets ΔE^{r}_{N} = 17 400 ± 1800 cm^{-1} for the lowest energy transition with **r** = (0,1,0). The corresponding energies for other **r** are shown in Table IV. Approximate values for the higher energy CT transitions can be obtained from these energies by adding the orbital energy gaps described above. The entries in parentheses in Table IV are obtained by fitting the experimental absorption spectrum as described in the following section.

The results collected in Table IV indicate that the CT transition with the lowest energy involves reduction of the molecule at (1,0,0), which is located immediately above the electron donor in Figure 2. However, this transition makes only minor contributions to the crystal's spectroscopic properties, because the matrix elements that connect it to the intramolecular transitions are relatively small (Table II). The more important CT transitions in which an electron is transferred to a molecule at (0,1,0), (0,−1,0), (1,1,0), or (−1,−1,0) are calculated to lie between 1000 and 3000 cm^{-1} above the transition for **r** = (1,0,0).

Calculated Spectroscopic Properties. The spectroscopic properties of the crystal can be calculated straightforwardly after diagonalization of **U**.[1,2,12] Because the CT transitions mix strongly with Q_y excitonic transitions (Table II), the calculated position of the long-wavelength absorption band depends critically on the energies of the CT transitions. As was discussed above, the main uncertainty in estimating these energies probably arises in the solvation energies for the MeBPh radicals in solution (ΔG^{w}_{sol}), which enter into the calculation of the orbital energy differences (α_N). Figure 3 shows how the calculated wavelength and dipole strength of the long-wavelength absorption band change if $\alpha_{\phi 2,\phi 3}$ is varied in the region around its calculated value. The wavelength matches the experimental result (862 nm) if $\alpha_{\phi 2,\phi 3}$ is put at about 38 200 cm^{-1}, so that the CT transition with **r** = (0,1,0) has an energy of 17 000 cm^{-1}. The optimum value of $\alpha_{\phi 2,\phi 3}$ is within the uncertainty range of the value obtained by using the adiabatic-charging treatment of the solvation energies (38 600 ± 1800 cm^{-1}). The adjusted CT transition energies are given as the final column in Table IV and are included in Table II for r = (0,1,0).

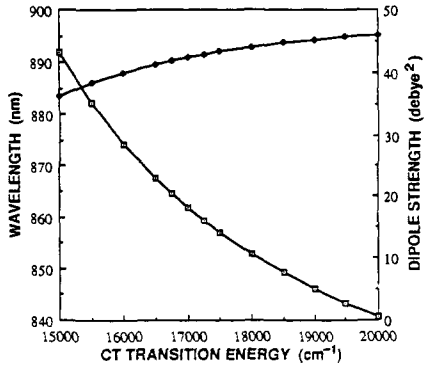

Figure 3. Calculated wavelength (□) and isotropic dipole strength (◆) of the lowest energy absorption band in the MeBPh crystal, as a function of the energies of the CT transitions. The abscissa gives the diagonal energy of the CT transition with **r** = (0,1,0) and N = (ϕ_2,ϕ_3), which is varied by changing the orbital energy difference, $\alpha_{\phi 2,\phi 3}$. The energies of the CT transitions with other values of **r** or N also shift in parallel with this energy, maintaining the spacing described in the text and in Tables II and IV. The other matrix elements are held constant at the values given in the text and Table II. The calculations include the 40 CT transitions involving the 10 different electron acceptors listed in Table IV. The calculated energy of the [(0,1,0), (ϕ_2,ϕ_3)] CT transition is 17 400 cm^{-1} (Table IV), which puts the long-wavelength absorption band at 858 nm. Decreasing the CT transition energies by 400 cm^{-1} moves the absorption band to 862 nm.

With the adjusted CT energies, the long-wavelength absorption band is calculated to have a dipole strength of 42.5 D^2, which is slightly larger than the dipole strength of the Q_y band of bacteriopheophytin *a* in solution (39 D^2 (ref 12)). The calculated value refers to the isotropic dipole strength that would be measured with a microcrystalline powder sample and unpolarized light. The strongest bands in the visible region of the spectrum are calculated to occur near 518, 520, 536, and 550 nm and to have isotropic dipole strengths of about 0.7, 1.0, 1.2 and 2.5 D^2, respectively. The first three of these bands are composed largely of the Q_x exciton transitions with some contributions from other excitonic and CT transitions; the 550-nm band is primarily a CT band. The weakness of the Q_x bands is consistent with the hypochromism seen experimentally in this region of the spectrum.[6] As has been discussed previously for the case of a bacteriopheophytin dimer,[12] the hypochromism in the Q_x region can be attributed to a strong interaction with the B_x transition (Table II). The Q_y exciton bands experience hyperchromism as a result of interaction with the B_y transition, but some of their dipole strength is borrowed by CT transitions and moves to the 550-nm region. This intensity borrowing increases if the CT transitions are moved closer to the Q_y transition in energy (Figure 3).

Figure 4A–C shows calculated absorption spectra for light polarized parallel to the crystallographic **a**, **b**, and **c** axes. For comparison, Figure 4D shows an experimental spectrum of MeBPh in solution. Also shown are absorption spectra that were measured with crystalline MeBPh, by using light polarized parallel and perpendicular to a macroscopic orientation axis.[6] (Because the experimental absorption spectra were obtained with a crystal different from the one that was used for X-ray crystallography,[5] it is not possible to connect the experimental axis unambiguously with the crystallographic axes. The measurements also leave open the possibility that the two crystals differed structurally, although there is no reason to believe that this was the case.) In agreement with the experimental spectra, the calculated spectra for the crystal exhibit pronounced linear dichroism. The absorption bands at 862 and 378 nm are intense for light polarized parallel to the **b** axis but are essentially missing from spectra calculated for **a** or **c** polarization. Because the crystallographic axes are not orthogonal, the dipole strengths calculated for light polarized along the three axes do not sum to the isotropic strength. The 862- and 378-nm transition dipoles are approximately parallel to the N1–N3

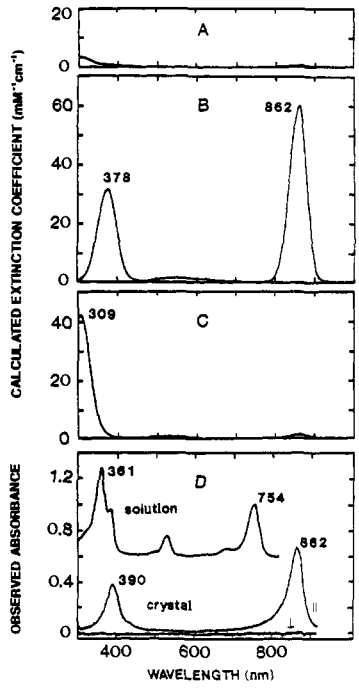

Figure 4. A–C: Calculated absorption spectra of the MeBPh crystal, for light polarized along the crystallographic **a**, **b**, and **c** axes, respectively. The energies of the CT transitions were adjusted as in Figure 3, so that the energy of the $[(0,1,0), (\phi_2,\phi_3)]$ transition was 17 000 cm^{-1}. Other matrix elements were as described in the text and Table II. For illustration, the calculated stick spectra were given asymmetric Gaussian band shapes.[1,2] D: Experimental absorption spectra of crystalline MeBPh measured with light polarized parallel (middle curve) and perpendicular (bottom curve) to a macroscopic orientation axis and of monomeric MeBPh in CH_2Cl_2–benzene solution (upper curve).[6]

molecular axis (see Figures 1 and 2).

The calculated spectra include a band near 309 nm that is strongest for light polarized along the **c** axis and very weak for **a** or **b** polarization (Figure 4C). This band was not seen experimentally (Figure 4D), possibly because the actual shift of the B_x exciton band to higher energies is larger than calculated. The observed red-shift of the B_y exciton band to 390 nm also is somewhat larger than the calculated shift to 378 nm. These discrepancies could reflect the neglect of dispersion effects on the diagonal transition energies or approximations inherent in our treatment of the intramolecular B_x and B_y transitions. As was noted previously,[1,12] the monomeric molecule's absorption bands in this region include several overlapping transitions that are represented only approximately by the simple set of configurations that we have used.

Discussion. Overall, the calculated absorption spectra for the MeBPh crystal agree remarkably well with the experimental measurements. This agreement was achieved by adjusting the single parameter, the gas-phase orbital energy difference $\alpha_{\phi 2,\phi 3}$ that enters into the calculation of the diagonal CT transition energies. Adjusting the orbital energy gap could, of course, compensate for errors in terms that were not treated as free parameters. However, it is encouraging that the CT transition energies that are needed to bring the calculated spectroscopic properties into alignment with experiment are within 400 cm^{-1} of the energies that were calculated directly from the crystal structure. Changing $\alpha_{\phi 2,\phi 3}$ by this amount shifts the crystal's long-wavelength transition by only 4 nm (Figure 3), so that even without this adjustment the agreement with experiment seems excellent.

Although our treatment is semiempirical in nature, it is important to note that we have not adjusted any of the parameters other than $\alpha_{\phi 2,\phi 3}$ for the particular problem of crystalline MeBPh. The QCFF/PI treatment that provided the molecular orbital coefficients, the atomic charges, and the atomic resonance and repulsion integrals used parameters that were obtained in earlier studies of other conjugated, heteroatomic molecules.[10] The configuration-interaction coefficients, the diagonal transition energies of the intramolecular transitions, and the redox potentials were derived from the experimentally measured properties of monomeric MeBPh or bacteriopheophytin a in solution.[1,6,12,15] The atomic polarizabilities and the bulk dielectric constant ϵ_0 that enters into the calculation of V^r_{bulk} were evaluated in previous studies of electrostatic interactions in proteins and solution.[16-18] The screening factor d in eq 25 was obtained by using an iterative, self-consistent procedure[16,17] to calculate V^r_{ind} for the crystal.

In principle, it would be attractive to replace any semiempirical molecular orbital treatment with ab initio calculations. This is not yet possible for systems of the size that we have considered here. Even for systems the size of an individual MeBPh molecule, available ab initio methods generally require an arbitrary scaling of the calculated energies, so that in the end they are no less empirical than treatments of the sort that we have used. When ab initio calculations on the individual molecules have been refined, they could readily be incorporated into a treatment of crystals along the lines discussed above.

The present theory can be tested more exhaustively by examining crystals of other related molecules. The general approach thus appears to be reasonable and seems likely to provide a powerful method for analyzing the quantum mechanical properties of complex, multimolecular systems. This result lends support to attempts to calculate the free energy gaps and electronic interaction energies that determine the dynamics of electron transfer in the photosynthetic reaction center.[14]

Acknowledgment. We thank Dr. J. Fajer for helpful discussion and for information on the crystal structure. This work was supported by grants from the National Science Foundation Research (PCM-8616161) and the National Institutes of Health (GM-40283).